

Supporting Information

**Design and fabrication of flexible glucose sensing platform
toward rapid battery-free detection of hyperglycaemia**

Hajime Fujita^a, Kento Yamagishi^b, Wenshen Zhou^c, Yu Tahara^d, Shao Ying Huang^c,
Michinao Hashimoto^{b,c}, Toshinori Fujie^{a,*}

^aSchool of Life Science and Technology, Tokyo Institute of Technology, 4259 Nagatsuta-cho, Midori Ward, Yokohama, Kanagawa 226-0026 (Japan), ^bDigital Manufacturing and Design (DManD) Centre, Singapore University of Technology and Design, Singapore 487372 (Singapore), ^cPillar of Engineering Product Development, Singapore University of Technology and Design, Singapore 487372 (Singapore), ^dDepartment of Physiology and Pharmacology, School of Advanced Science and Engineering, Waseda University, Wakamatsu-cho 2-2, Shinjuku-ku, Tokyo 162-8480 (Japan).

*Corresponding authors:

T. F: t_fujie@bio.titech.ac.jp, Tel: +81-45-924-5712

This file includes:

Supporting Figures S1 to S10

References

Supporting Figures

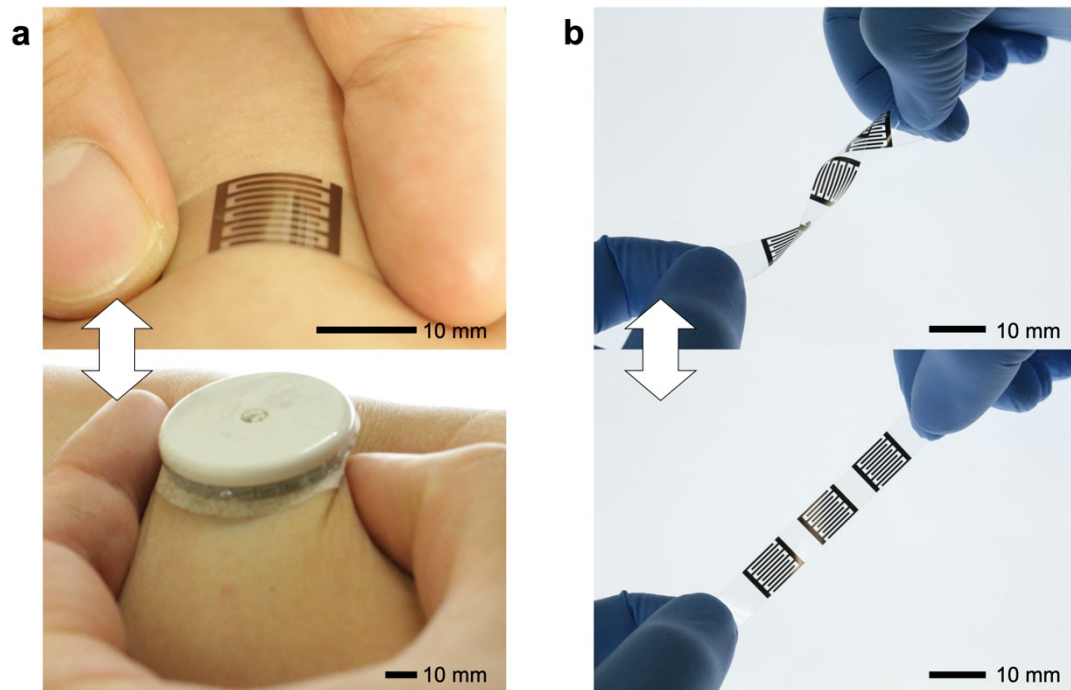


Fig. S1 Conformability of the developed sensor to biological tissues and living bodies and mechanical durability. (a) Comparison of body conformability between our sensing element (top) and Freestyle Libre, a commonly used continuous glucose monitoring device (bottom). (b) Mechanical durability of sensing element under repeated deformation.

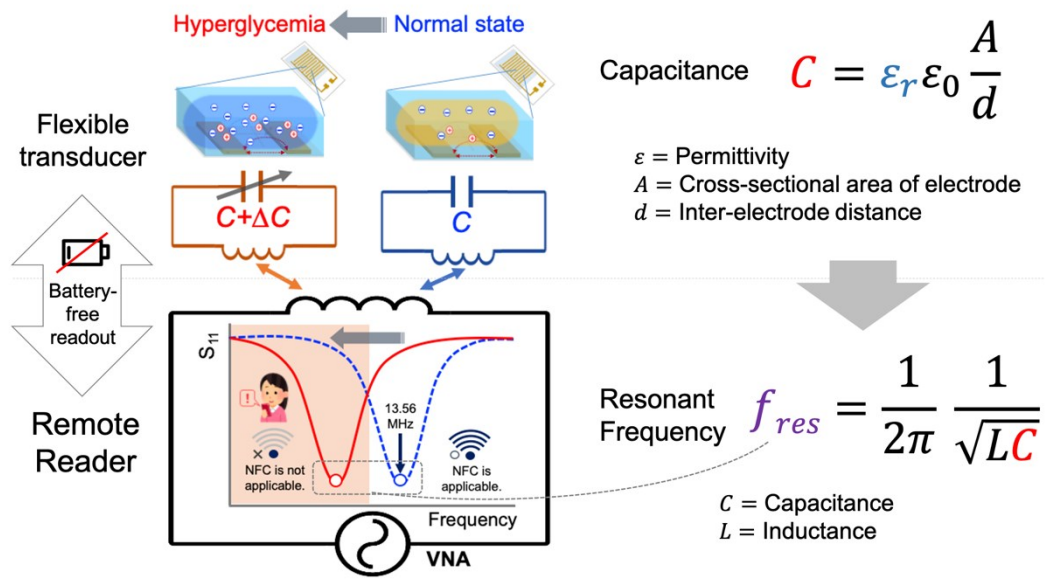


Fig. S2 Schematic diagram of glucose sensing based on the change in capacitive component and the resulting shift in resonant frequency.

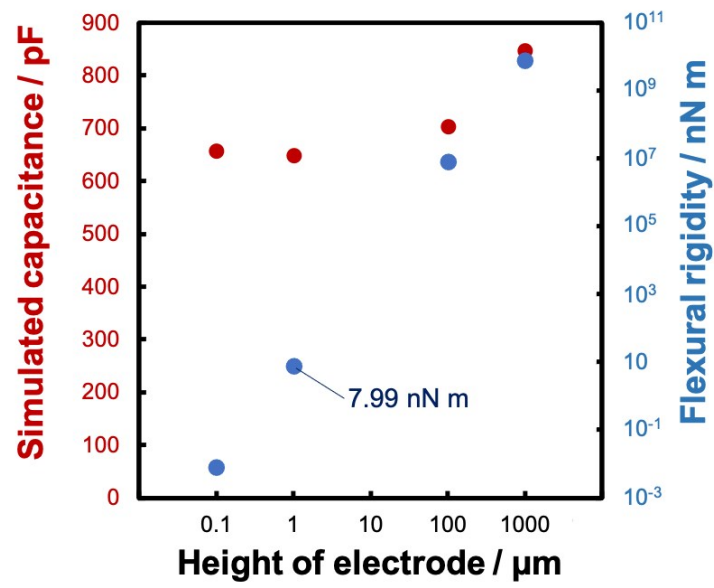


Fig. S3 Relationship between the height of electrode and the simulated capacitance (first y-axis, surrounding dielectric material: water (relative permittivity: 80)), and flexural rigidity of electrode (second y-axis).

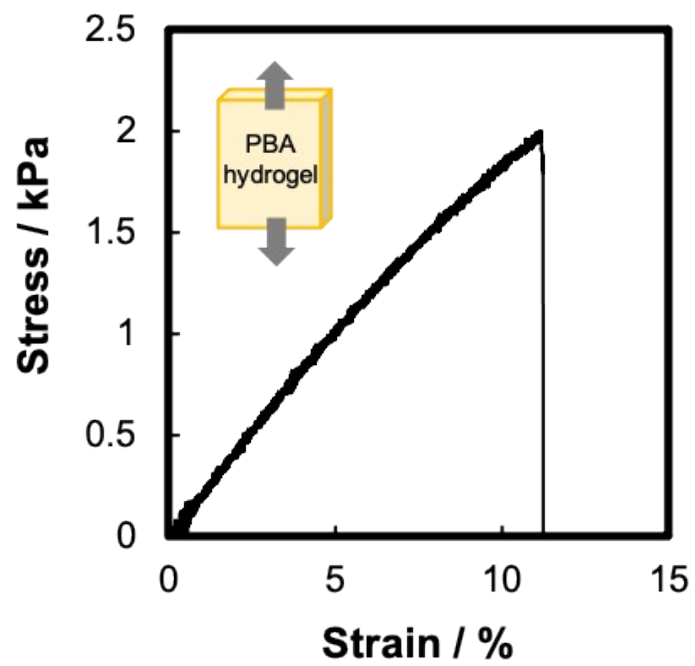


Fig. S4 Stress-strain curve of PBA hydrogel for calculating of the Young's modulus.

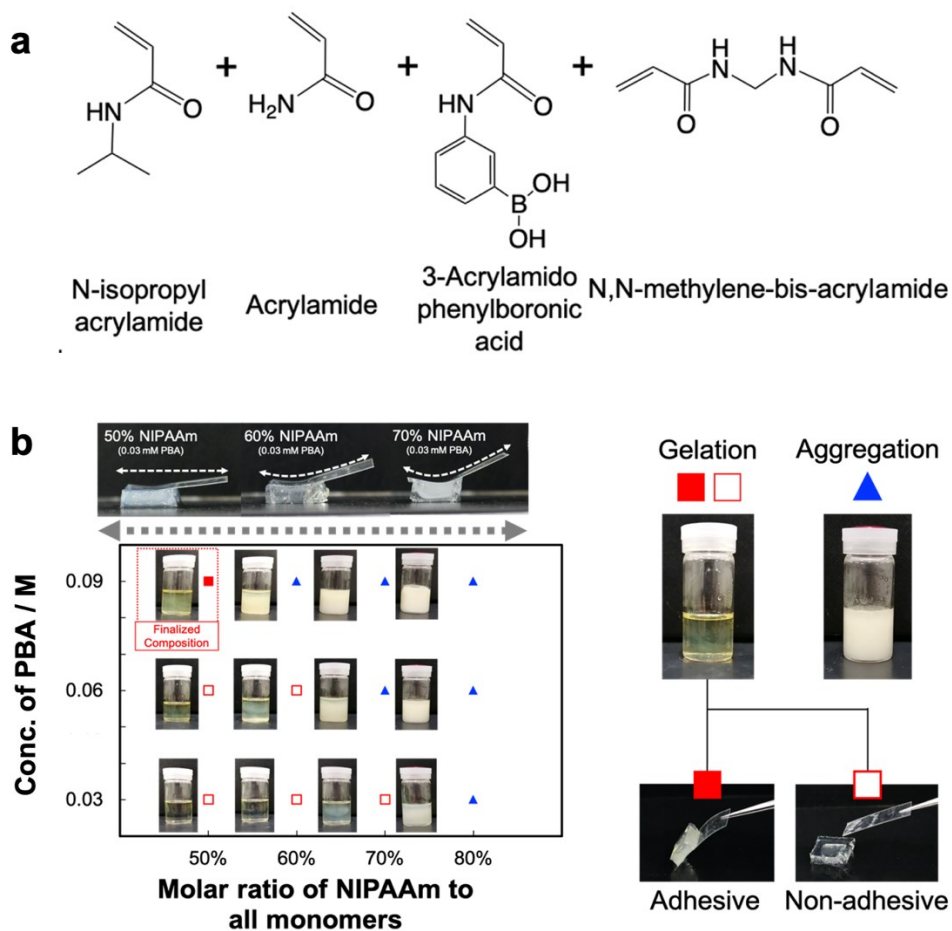


Fig. S5 Composition of the phenylboronic acid hydrogel. (a) Chemical structure of monomers contained in glucose-responsive PBA hydrogel. (b) Relationship between the fraction of NIPAAm and the concentration of PBA.

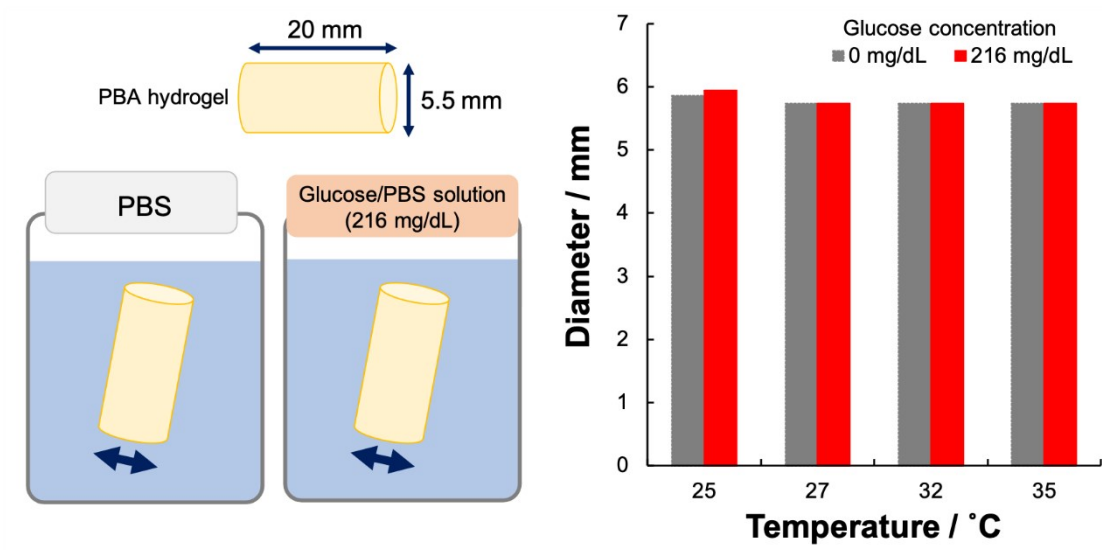


Fig. S6 Relationship between the temperature and the diameter of cylindrical PBA hydrogel (initial diameter: 5.5 mm, length: 20 mm) in PBS and PBS supplemented with glucose (216 mg/dL).

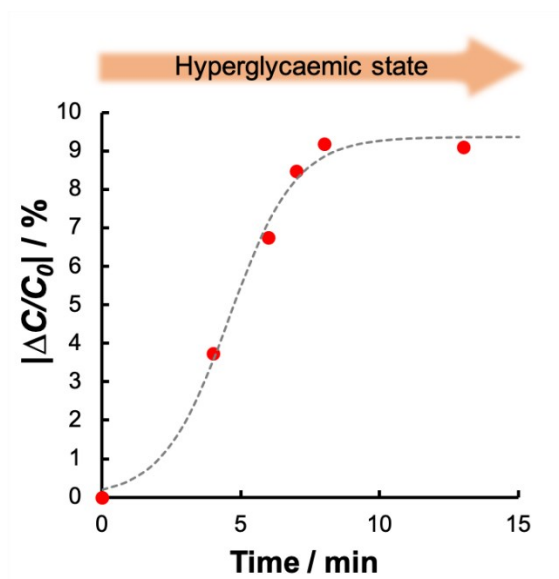


Fig. S7 Response of capacitance to PBS supplemented with glucose (216 mg/dL) (Measured frequency: 13.56 MHz).

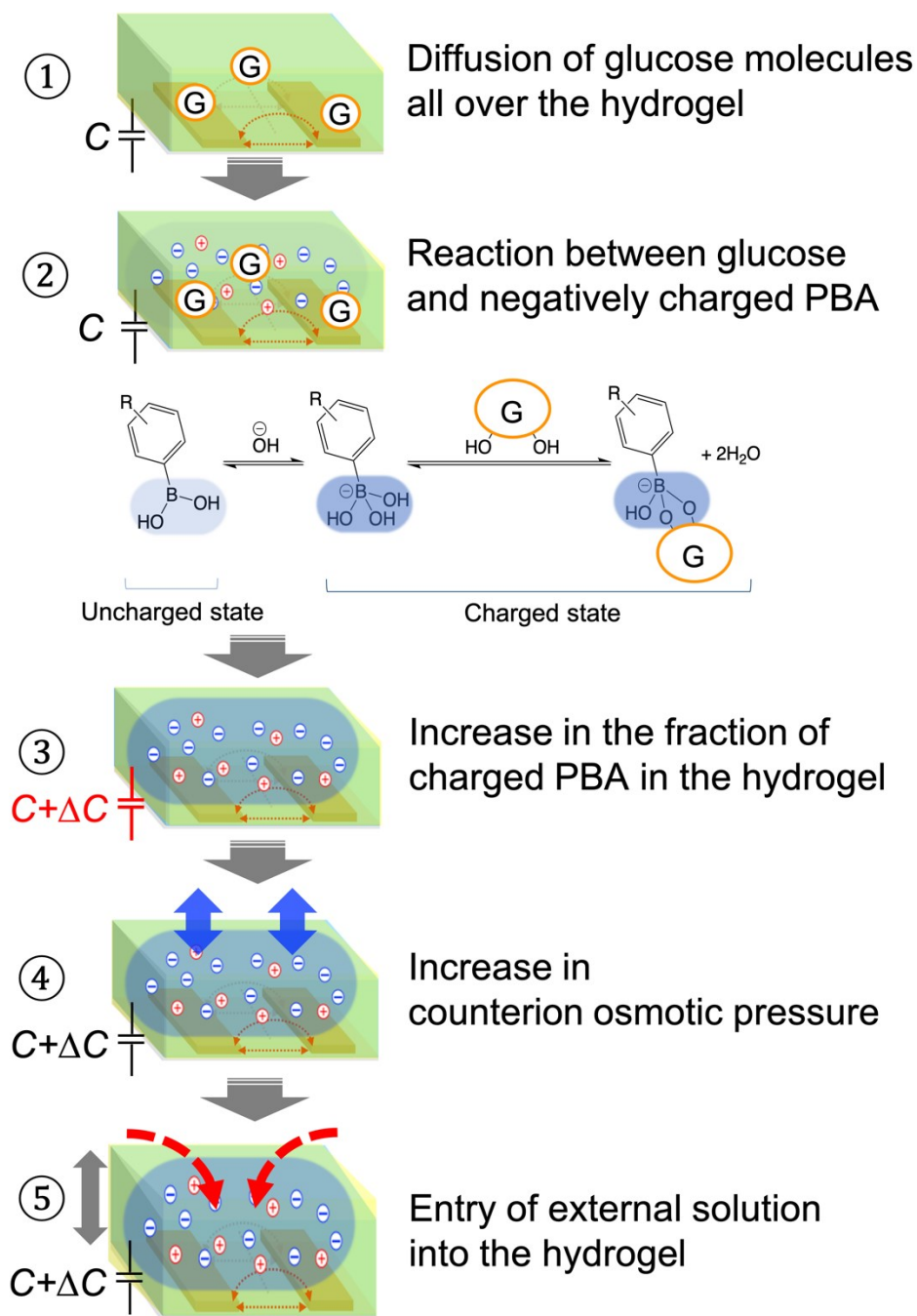


Fig. S8 Mechanism of the reaction between glucose and phenylboronic acid and the capacitive response in phenylboronic acid (PBA) hydrogel.

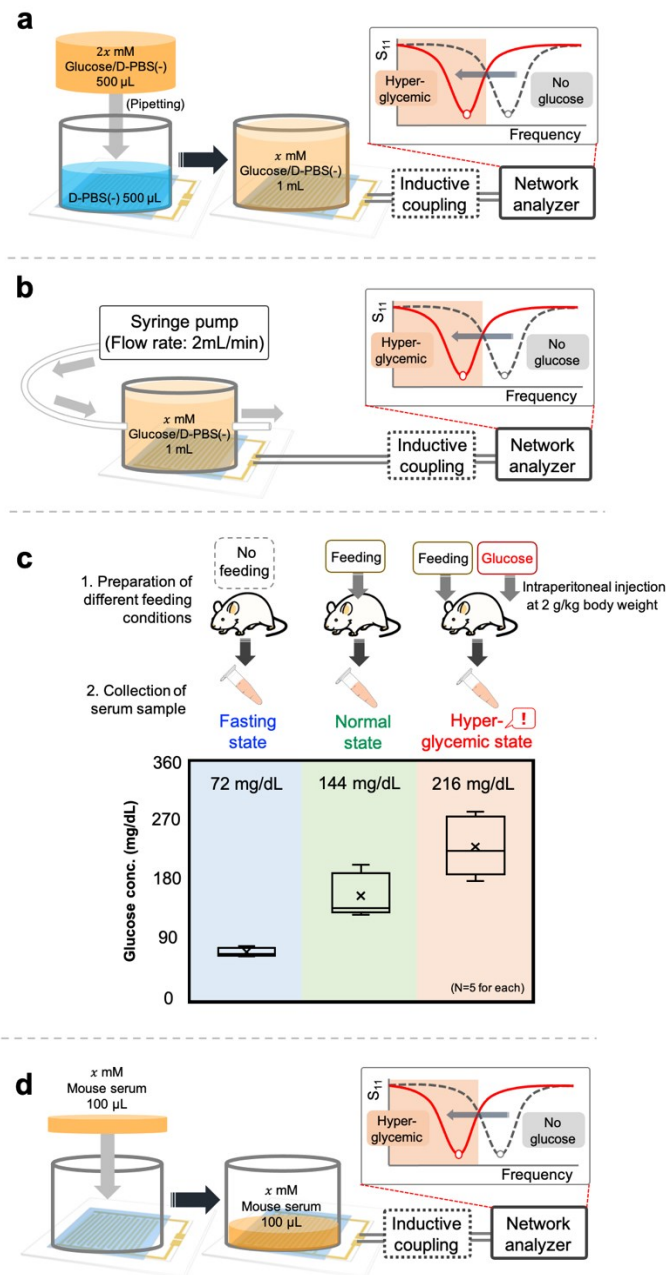


Fig. S9 Experimental setups for battery-free detection of hyperglycemia. Experimental procedure for demonstrating (a) *in-vitro* battery-free detection and (b) reversible response of sensor (in terms of resonant frequency). (c) Experimental procedure for preparing three types of glucose concentration of mouse serum: hypoglycemic, normoglycemic, and hyperglycemic levels (N=5 for each type). (d) Experimental procedure for demonstrating *ex-vivo* battery-free detection.

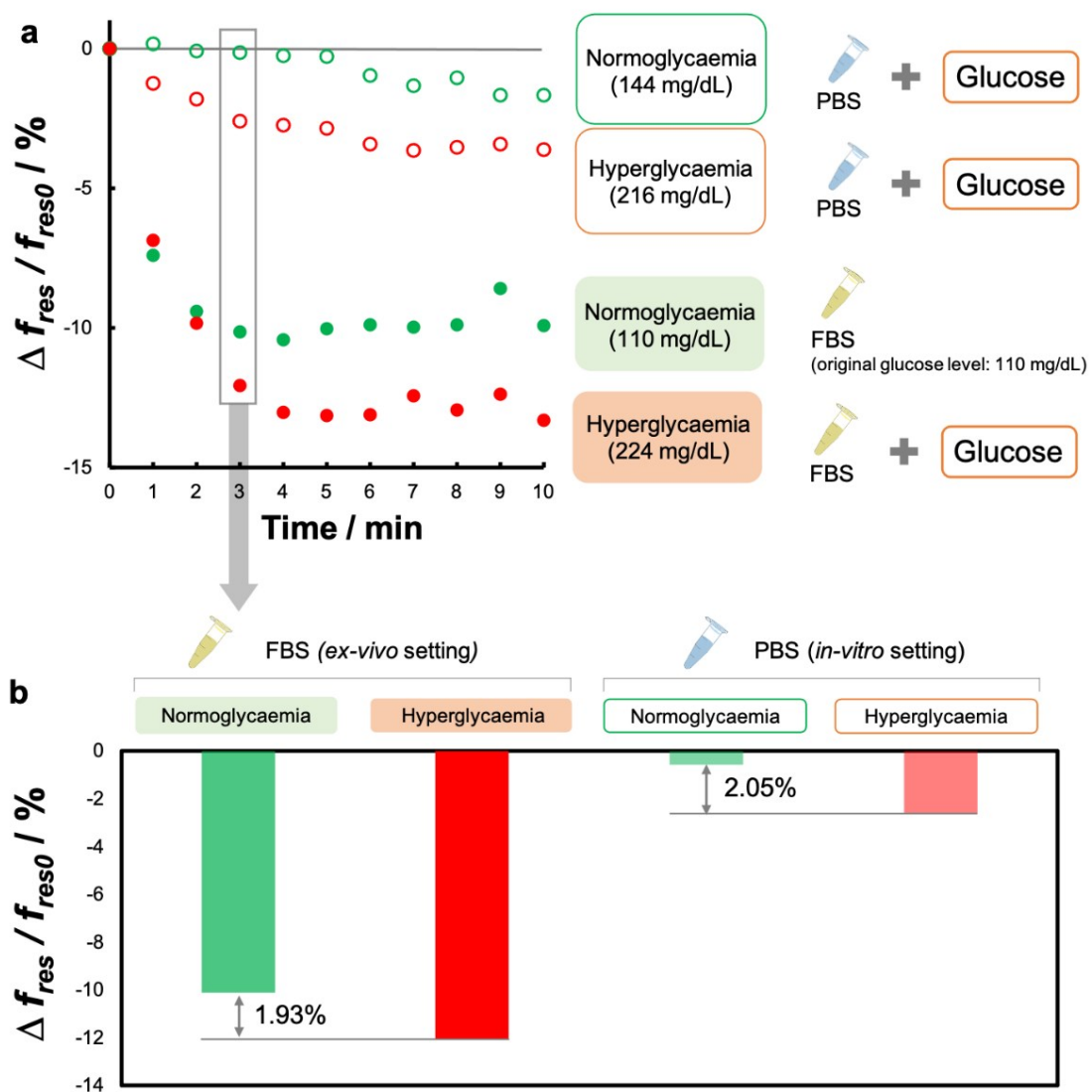


Fig. S10 Analysis of sensor response to the changes in glucose concentration using fetal bovine serum (FBS). (a) Time course of sensor response to FBS or PBS supplemented with glucose (closed red circle: response to FBS supplemented with hyperglycaemic level of glucose (224 mg/dL), closed green circle: response to FBS supplemented with normoglycaemic level of glucose (110 mg/dL), open red circle: response to PBS supplemented with hyperglycaemic level of glucose (216 mg/dL), open green circle: response to PBS supplemented with normoglycaemic level of glucose (144 mg/dL)). (b) Comparison of sensor response in 3 min to glucose solution in FBS or PBS. The difference of shift in resonant frequency between normoglycaemia and hyperglycaemia is 1.93% for FBS supplemented with glucose and 2.05% for PBS supplemented with glucose.